

Characterization of CEST effect from Glucose In Vitro

Sai Chilakapati¹, Sanjana Reddy¹, Mohammad Haris¹, Anup Singh¹, Kejia Cai¹, Kavindra Nath², Hari Hariharan¹, and Ravinder Reddy¹

¹Radiology, University of Pennsylvania, Philadelphia, Pennsylvania, United States, ²Molecular Imaging Lab, University of Pennsylvania, Philadelphia, Pennsylvania, United States

Introduction:

Glucose is the most abundant and common source of energy. Various diseases have been linked to the bodies' inability to maintain glucose homeostasis, like diabetes, and changes in glucose metabolism have been linked to the outbreaks of various metabolic as well as neurological diseases. Currently, the methods for mapping glucose utilization and concentrations are limited and each has its own major drawbacks. Positron emission tomography (PET) is widely available techniques to measure the glucose uptake rate using a radioactive tracer i.e. 6-fluoro-deoxy-glucose (FDG), a radioactive analog of glucose, in order to map glucose utilization¹. However, this technique has very low spatial resolution (>3 mm) and requires exposure to radiation for a long time. Similarly Paramagnetic chemical exchange saturation transfer (PARACEST) is a technique that requires the injection of paramagnetic substance that binds to glucose in order to amplify the signal². Though it is successful in imaging glucose concentrations, the paramagnetic substances are known to be toxic at high levels. Both the Proton and ¹³Carbon MRS has been used to study glucose metabolism, but are limited to low resolution^{3,4}. The various other techniques that exist are invasive and require the use of implantable devices that detect glucose concentrations either electrochemically, optically, enzymatically, or by microdialysis. The effect that results from the transfer of saturated magnetization from exchangeable protons to bulk water is commonly known as chemical exchange saturation transfer (CEST). This technique has been earlier employed to image the various metabolites and macromolecules *in vivo*⁵⁻⁷. However, the CEST effect from glucose has been shown earlier between 1-3 ppm using non-physiological concentration of glucose (>10 mM). In the current study, we characterized the CEST effect from glucose at brain physiological concentration (<10 mM) at different saturation pulse power and saturation duration and image them at high spatial resolution *in vitro*.

Materials and Methods:

High Resolution ¹H NMR Spectroscopy: High resolution NMR spectroscopy from 200mM glucose solution was performed on 9.4T vertical bore (Varian, Palo Alto, CA) scanner at two different temperatures (10, and 37 °C) with a single pulse-acquire spectroscopy with TR = 4 s, number of averages = 64.

CEST Imaging: Glucose solutions of varying concentrations, 2, 4, 6, 8, and 10 mM, were prepared in phosphate buffer saline (PBS) and adjusted to a pH 7.0. These samples were added to small test tubes (10mm diameter), and immersed inside a large PBS phantom. CEST imaging was performed on 7T Siemens whole body MRI scanner (Siemens Medical Systems, Erlangen, Germany) using a single channel circular polarized transmit-receive head coil. During the course of experiment temperature was maintained at 37±1°C using a custom designed styrofoam chamber. A special optimized saturation pulse train was used with 10 Hanning windowed rectangular pulses of 100 ms duration each with a 200 μ s delay between them. The saturation pulse excitation bandwidth was 5 Hz for 1 s pulse with 1% bandwidth of 20 Hz. The total repetition time of the sequence was adjusted to stay within SAR limits. The sequence parameters were: slice thickness = 10 mm, GRE flip angle = 10°, GRE readout TR = 8.8 ms, TE = 4.3 ms, field of view = 100 × 100 mm², matrix size = 192 × 192, and one saturation pulse and 64 segments acquired every 10 s. CEST images from 0.7 to 1.3 ppm were collected in step size of 0.1 ppm at different saturation pulse power ($B_{1\text{rms}}$) (93, 124, 155 and 186 Hz) and saturation duration (0.5, 1, 2 and 3 s). The B_0 and B_1 maps were also gathered. CEST maps were computed using the equation $\text{CEST} = 100 * [(S_{-ve} - S_{+ve})/S_0]$. where S_{-ve} and S_{+ve} are the B_0 corrected MR signals acquired while saturating at -1 p.p.m., +1 p.p.m from water resonance, while S_0 is the image obtained without application of any saturation pulse. The CEST contrast map was further corrected for any B_1 inhomogeneity.

Results and Discussion:

The high resolution ¹H NMR spectra showed the clear resonance from -OH group (~1 ppm) of glucose at low temperature which broadened at 37 °C due to exchange broadening (Fig. 1). Earlier, the -OH resonance from glucose has been shown between 1-3 ppm⁵. The exchange rate (k_{ex}) of the -OH proton is reported around 1000 s⁻¹¹⁵, which is under slow to intermediate exchange rate at 7T ($\Delta\omega = 1.8 \times 10^3$ rad/s) and satisfy the condition to obtain the CEST effect ($k_{ex} < \Delta\omega$). The graphs shown in figure 2 depict the CEST contrast from glucose at different $B_{1\text{rms}}$ and saturation duration. Both increase in $B_{1\text{rms}}$ and saturation duration resulted in increased CEST contrast from glucose. A linear relationship between glucose concentration and CEST contrast is observed at all $B_{1\text{rms}}$ and saturation duration. The CEST map as shown in figure 3 shows the CEST contrast from different concentration of glucose at $B_{1\text{rms}}$ of 186 Hz and 3s saturation duration. The next step is to monitor the change in the brain glucose concentration after intravenous injection of glucose using the optimized saturation parameters. Further work in these lines is in progress in our departments.

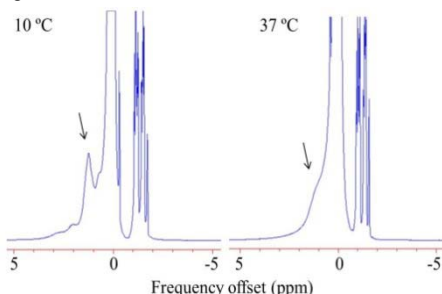


Figure 1: High resolution ¹H NMR spectra clearly show the glucose -OH proton resonance at ~1 ppm at lower temperature which broadened at higher temperature due to exchange broadening.

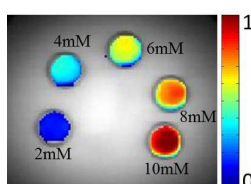
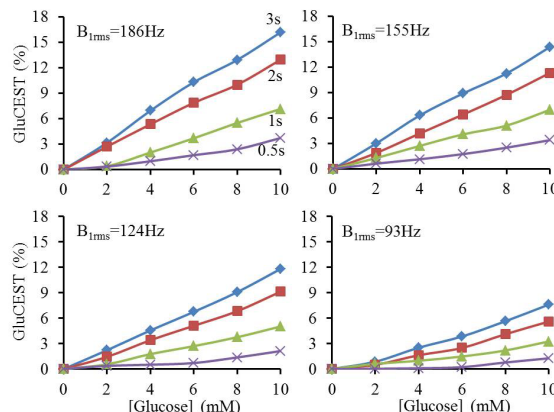


Figure 3: CEST map at 1 ppm from different concentration of glucose obtained using $B_{1\text{rms}}$ of 186 Hz and 3s saturation duration.



References:

1. Phelps ME et al. Ann Neurol 6: 371-88, 1979.
2. Ren J et al. Magn Reson Med 60:1047-55, 2008.
3. van Zijl PC et al. Magn Reson Med 30:544-51, 1993.
4. de Graaf RA et al. PNAS 101:12700-5, 2004.
5. van Zijl PC et al. PNAS 104:4359-4364, 2007.
6. Haris M et al. Neuroimage 2011;54:2079-85.
7. Cai K et al. Nature Medicine (In press)

Figure 2: Shows the $B_{1\text{rms}}$ and saturation duration dependent CEST contrast at 1ppm from different concentration of glucose (2, 4, 6, 8, and 10 mM). Increase in CEST contrast is observed with increased $B_{1\text{rms}}$ and saturation duration. A linear relationship between glucose concentration and CEST contrast is observed at all $B_{1\text{rms}}$ and saturation duration.

Acknowledgements:

This work was performed at NCRR supported Biomedical Technology and Research Center (P41 RR02305).